January 2013

Characteristics of Interface between MgAl2O4 Spinel and CaO-Al2O3-SiO2-MgO Slag

H Abdeyazdan
University of Wollongong, ha984@uowmail.edu.au

M A. Rhamdhani
Swinburne University

N Dogan
University of Wollongong, ndogan@uow.edu.au

M Chapman

B J. Monaghan
University of Wollongong, monaghan@uow.edu.au

Characteristics of Interface between MgAl2O4 Spinel and CaO-Al2O3-SiO2-MgO Slag

Keywords

spinel, cao, al2o3, sio2, mgal2o4, mgo, between, slag, interface, characteristics

Publication Details

Abdeyazdan, H., Rhamdhani, M. A., Dogan, N., Chapman, M. & Monaghan, B. J. (2013). Characteristics of Interface between MgAl2O4 Spinel and CaO-Al2O3-SiO2-MgO Slag. Proceedings of the 3rd Indonesian Iron and Steel Conference (pp. 144-159). Bandung, Indonesia: Instutut Technologi Bandung.

Characteristics of Interface between $MgAl_2O_4$ Spinel and $CaO-Al_2O_3-SiO_2-MgO$ Slag

H. Abdeyazdan[1], M.A. Rhamdhani[2], N. Dogan[1], M. Chapman[3], B.J. Monaghan[1]

[1]PYROmetallurgical Research Group, University of Wollongong, Australia
[2]HTP Group, Swinburne University of Technology, Melbourne, Australia
[3]BlueScope Steel, Ltd, Port Kembla, Australia

Abstract

Inclusion type and concentration in steel is critical in steelmaking, affecting both productivity through clogging, and downstream physical properties of the steel. They are normally removed from steel by reacting with a slag phase. For efficient inclusion removal the inclusions must attach/bond with the slag phase. The strength of the attachment can be characterized by the wettability of the slag on the inclusions. In this study, the interface characteristics between solid spinel ($MgAl_2O_4$) with low porosity of 1.9% and ladle slags of the $CaO-Al_2O_3-SiO_2-MgO$ were investigated, in particular the contact angle was measured at 1500 °C using a modified sessile drop technique for different CaO/Al_2O_3 mass percent ratios ranging from 0.98 to 1.55. Characteristic curves of wettability (θ) versus time showed a rapid decrease in wetting in the first 10s tending to a plateau value at extended times. The chemical interaction at the interface between spinel ($MgAl_2O_4$) and slag was analyzed by carrying out detailed thermodynamic evaluation and characterization using scanning electron microscopy/energy dispersive spectroscopy (SEM/EDS). There is evidence of the slag penetrating the substrate via pores and along grain boundaries, forming a penetration layer on the substrate. The depth of the penetration layer was found to be a function of cooling rate. It decreased from ~190μm to ~50μm for a slow cooled slag-spinel substrate sample in the furnace to a rapidly cooled slag-spinel substrate sample respectively

Keywords: inclusion removal; wettability; clean steel

I. Introduction

Inclusion control and removal from steel is key in the production of high quality steel[1]. Inclusions are usually formed during steel deoxidation process, though they may also result from slag and mould flux entrainment, refractory degradation or precipitation events on steel solidification. They are generally removed to the slag phase[2]. In the removal process the inclusions contact and bond/react with the slag phase then dissolve in the slag. If the bond is weak, then local fluid conditions are likely to result in the shearing of the inclusion-slag bond and the inclusions remain in the steel. The strength of the inclusion bond or reactivity with slag may be assessed by measuring the dynamic wetting

of the slag on a substrate made of the inclusion phase[3]. Research on inclusion removal in steel refining is principally divided into categories of flotation of inclusion to the steel/slag interface[4-5], modification to improve reactivity/separation with the slag phase[6] and dissolution in the slag phase[7-13].

A number of studies relevant to inclusion dissolution in slags have been carried out on bulk refractory or ceramic materials[14-18] where the material is dipped in slag and held for a period of time, removed, then analyzed for slag corrosion and/or penetration. Some recent studies have used high temperature microscopy offering the possibility of analyzing the dissolution behavior of a single inclusion in a slag directly [7-13]. Monaghan and Chen[7] and Valdez et al.[12] used high temperature microscopy to investigate the effect of slag basicity on spinel inclusion dissolution. They found that the rate of dissolution of the spinel particles increased with increasing basicity of the slag.

While it is understood that inclusion-slag interfacial tension/wetting play a critical role in inclusion removal, there are limited data of slags on typical inclusion phase types in the literature. Recently the current authors[3] have investigated dynamic contact angle (θ) of slags in the CaO-Al_2O_3-SiO_2-MgO system on a ceramic representing an $MgAl_2O_4$ spinel-type inclusion using the sessile drop technique. For slags with CaO/Al_2O_3 mass ratios, noted C/A, of between 0.98 and 1.55, it was found that over the first 30 seconds of contact of the slag on spinel substrate that θ rapidly decreased from ~40° to ~15°. Further, there was not a clear relationship between θ and the C/A of the slag and that the slag penetrated the spinel substrate. The spinel substrates used had a high porosity of ~6.7%. It was not clear if the penetration was simply a result of the relatively high porosity sample and/or a function of the time the samples spent in the furnace. More specifically did the slag penetration happen during the measurement or as a result of the slag/substrate remaining in the hot zone of the furnace as it cooled.

To address the uncertainty due to porosity/penetration issues the dynamic contact angles reported in 6.7% study[3] have been repeated using higher density spinel substrates.

II. Experimental

A schematic of the modified sessile drop apparatus used to measure the contact angle in this study is given in **Figure 1**. The slag and substrate were heated separately to 1500 °C, the experimental temperature, under high purity of (99.99%) argon at a flow rate of 0.75 l/min. The gas was scrubbed by passing through ascarite and drierite prior to entering the furnace. Once the temperature has stabilised (~10 minutes) the slag is added to the spinel substrate. A novel method of place the slag on the surface of the ceramic substrate has

been developed. The solid slag is held in the Pt wire loop (number 4 in **Figure 1**). As it melts and becomes liquid it remains held in the Pt wire by interfacial forces until thermal stabilization is reached. The slag is then contacted/added to the substrate. This technique allows the addition of slag in liquid state at the target temperature and avoids the uncertainty of the time zero of the experiment (starting point of experiment).

Prior to carrying out the experiment the substrate was levelled in the furnace using an alignment laser. This is critical to minimise gravity affects distorting the liquid. To start the experiment, the alumina support rod (number 3 in **Figure 1**) was lowered so that the slag contacted the $MgAl_2O_4$ substrate. The moment at which the liquid slag is contacted to the substrate and separated from the Pt wire is defined as zero time. Approximately 0.1g of slag from an original 0.2 g was transferred to the substrate. The mass of slag added represents a compromise between errors associated with scale at small masses and using a mass that is less than the critical value of that required for gravity distortions of the droplet[20]. Once the slag is added the twin bore tube, alumina support and Pt wire were withdrawn to a cold part of the furnace chamber. The spreading of the slag on the substrate was recorded with a Sony 6.1 MP video camera (HDR-SR7E). The camera was fitted with a 2x telephoto lens and 2 HOYA neutral density filters (NDX4 and NDX400) in series. At the end of the experiment, after ~15 minutes at the experimental temperature after time zero, the slag and substrate were cooled in the furnace at a rate of ~7°C/min.

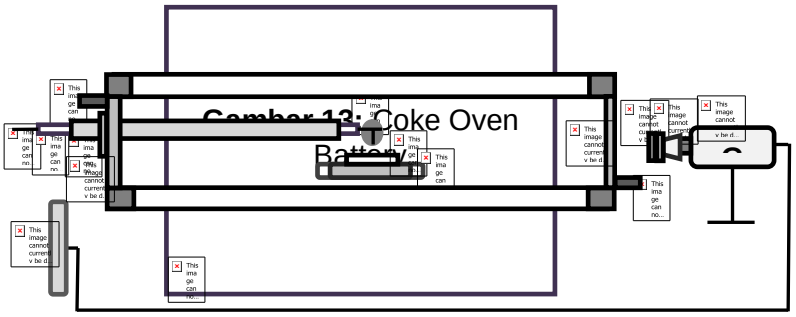

Figure 1 - A schematic of the sessile drop apparatus. 1: Pt Wire, 2: Twin bore tube, 3: Alumina support, 4: Liquid slag held by Pt wire, 5: Spinel substrate, 6: Tray and block, 7: Resistance furnace, 8: Inlet gas, 9: Outlet gas, 10: Camera, 11: 2x telephoto lens, 12: Filters, 13: Quartz window, 14: Monitor, 15: Flange

The contact angle (θ) was calculated using equation (1) and the geometry of a spherical cap as shown in **Figure 2** [20] from digital still images captured from the recordings,

$$\frac{\theta}{2} = \tan^{-1}\frac{h}{a} \qquad (1)$$

where R is the radius dissected by a base plane, h is the height of contact circle and a is radius of contact circle.

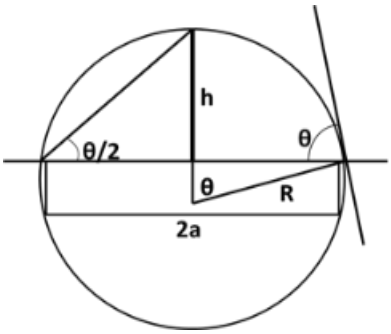

Figure 2 - Geometry of a sessile drop approximated by a spherical cap defined by radius of the base and height above basal plane.

The slags used were prepared by mixing laboratory grade oxides (CaO, Al_2O_3, SiO_2 and MgO) of appropriate proportions. These mixtures were then melted in a platinum crucible, quenched and crushed. This process was repeated twice to ensure slag homogeneity. Compositions of the resultant slag, as measured by XRF, are given in **Table 1**. C/A represents the mass% ratio of CaO/Al_2O_3. From these slags, 0.2g sintered pellets were prepared and used in the sessile drop experiments.

Table 1: Chemical composition of the experimented slags in mass%

Slag	CaO	Al_2O_3	SiO_2	MgO	C/A
1	41.8	42.7	9.2	6.3	0.98
2	46.3	37.1	9.8	6.8	1.25
3	50.9	32.9	9.5	6.7	1.55

The $MgAl_2O_4$ spinel powders were prepared from high purity laboratory grade MgO and Al_2O_3 (> 99%) starting materials by reaction sintering. These were mixed and then pressed into pellets and sintered at 1600 ˚C for 24 hours. This sintered material was then crushed to a fine powder (< 38µm) and re-sintered at 1725 ˚C for 6 hours. After the second sintering, the spinel phase was confirmed by X-ray diffraction (XRD). No other phases were identified via XRD. The substrates were then polished to 1µm for the sessile drop experiments. The substrates had an average apparent porosity[21] of 1.9% and a spinel composition of 71.7% Al_2O_3 and 28.3% MgO in mass%. Post experiment the sample was sectioned and prepared for electro-optical analysis. A JEOL–JSM6490 LV scanning electron microscopy (SEM) with energy dispersive spectroscopy (EDS) was

used. To assess the effects of time/cooling on penetration of the slag into the spinel substrate a further experiment was carried out using slag with a C/A ratio of 0.98. In this experiment the slag was added similarly the previous experiments. The primary difference was that 30 seconds after time zero, the furnace was opened and the slag-substrate couple was removed and left to rapidly cool in air on a laboratory bench. All other experimental conditions were the same as outlined for the furnace cooled samples. The total time this slag the slag-substrate couple remained in the hot zone of the furnace was ~60 s.

III. Results and Discussion

Figure 3 shows a typical example of the spreading and wetting behavior of a liquid slag drop on a spinel substrate is shown. It can be seen that the liquid drop spreads out on the substrate within a few seconds.

The results of the wetting behaviour for the slags are given in **Figure 4**. The data presented represent an average of a minimum of two runs per C/A ratio tested. The θ decreased from 37.7°, 28.7° and 27° at time zero for the C/A 0.98, C/A 1.25 and C/A 1.55 slags respectively to a slag C/A ratio independent value. After 30s, at the end of the experiment, the θ was ~18.1°. This value represents an average of all data reported. It would appear the rate of θ change in the early part of the experiment decreases with increasing C/A ratio. The significant drop in θ in the first 6s is consistent with the previous work the authors have reported on the higher porosity spinel material[3] and similar to what other workers found for $CaO\text{-}SiO_2\text{-}Al_2O_3$ based slags on alumina[22]. The initial drop in θ is likely to be principally due to the reaction of the slag with the substrate it may also contain a momentum component due to the slag addition technique.

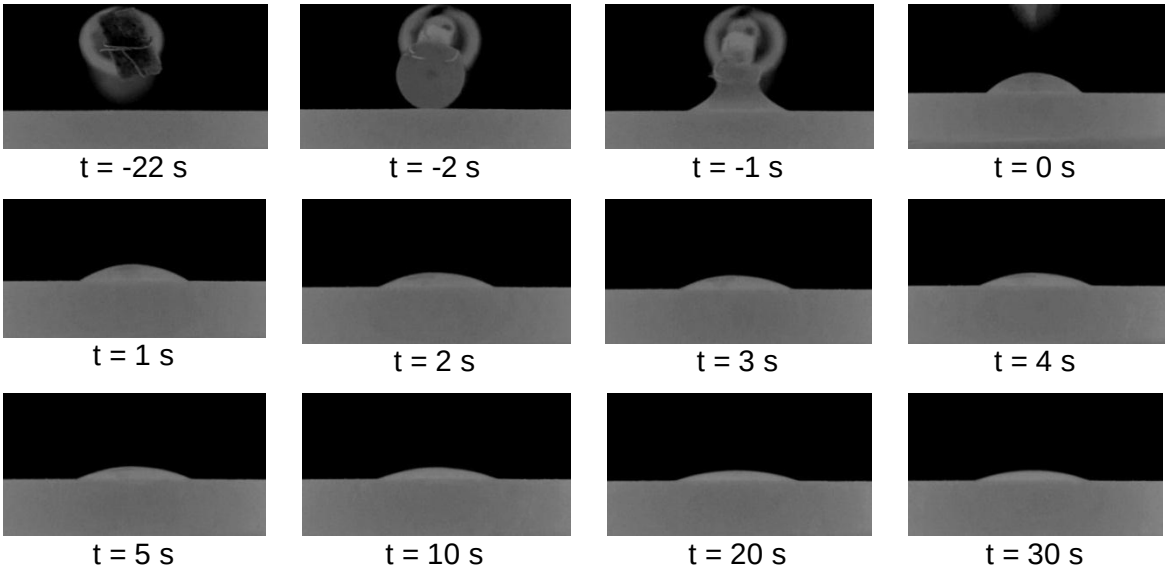

Figure 3: Spreading behaviour of the slag C/A 1.25 on the spinel substrate.

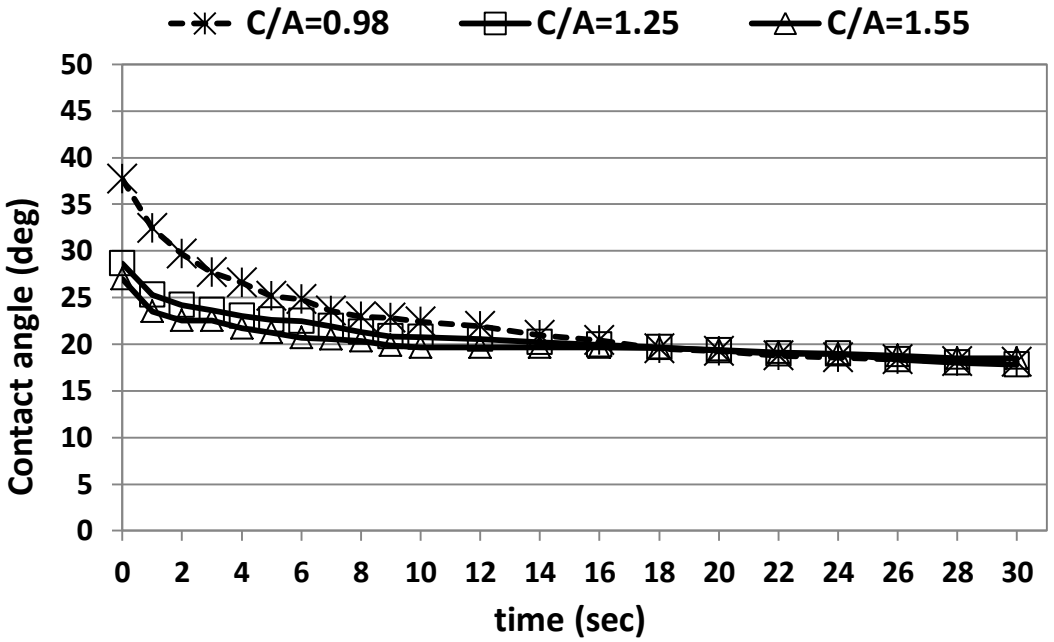

Figure 4: θ versus time measured for slags of different C/A ratios on a spinel substrate.

SEM characterization of the interface is given in **Figures 5a, 6a** and **7a** for the C/A 0.98, C/A 1.25 and C/A 1.55 slags respectively. Inspection of these figures shows a slag penetration layer at the interface between the slag and spinel substrate. Given the changes in θ it is likely this layer in part represents reaction between the slag and spinel substrate. It is also likely to contain a reactivity/penetration component that is associated with the cooling down period of the experiment. EDS analysis of the areas marked in **Figures 5a** to **7a** are given in **Table 2**. EDS spot analyses of the penetration layer shown in **Figures 5b, 6b** and **7b** are given in **Table 3**.

Table 2: EDS analysis of areas in Figures 5a, 6a and 7a. Values are in mass%

C/A	Location/Phases	CaO	Al_2O_3	SiO_2	MgO
0.98	Slag	43.3	41.7	9.0	6.0
	Penetration zone	6.3	65.4	3.4	24.9
	Spinel substrate	0.4	71.6	2.8	25.2
1.25	Slag	41.9	41.7	8.2	8.2
	Penetration zone	6.0	67.0	2.6	24.4
	Spinel substrate	0.2	72.0	2.8	25.0
1.55	Slag	44.0	42.0	6.6	7.4
	Penetration zone	6.3	66.2	3.1	24.4

	Spinel substrate	0.4	71.9	2.9	24.8

Table 3: EDS spot analysis of phases in Figures 5b, 6b and 7b. Values are in mass%

C/A	Location/Phases	CaO	Al_2O_3	SiO_2	MgO
0.98	Spinel (grey phases)	0.1	69.7	2.6	27.6
	Slag penetration (White phase)	42.6	47.0	7.6	2.8
1.25	Spinel (grey phases)	0.2	70.3	2.5	27.0
	Slag penetration (White phase)	36.7	58.4	2.1	2.8
1.55	Spinel (grey phases)	0.2	69.6	2.6	27.6
	Slag penetration (White phase)	43.0	41.2	9.9	5.8

From these data it would appear that the slag C/A 1.25 and 1.55 has become depleted of CaO and enriched with Al_2O_3. The composition of slag C/A 0.98 is similar to the starting slag composition given in **Table 1**. In the slag penetration layer there appears to be two phases. A dark phase representing something close to the original spinel and a white phase that most likely represents slag penetration into the spinel. From **Figures 5b, 6b** and **7b** it would appear the slag is penetrating through pores and along the grain boundaries.

Thermodynamic analysis of the slag-spinel substrate systems has also been carried out using MTData[19] and the isopleths representing spinel substrate-slag C/A 0.98 and 1.55 are given in **Figures 8a** and **8b** respectively. From **Figure 8a** it can be seen that at the experimental temperature (1500 ^oC) the spinel phase and oxide liquid (slag) phase are stable. In **Figure 8b** for the C/A 1.55 slag, spinel phase, oxide liquid (slag) and halite (MgO) phases are stable. The phases predicted are broadly consistent with the EDS analysis of the penetration layer that showed a two phase region. The darker phase being consistent with the original spinel and the white phase being consistent with the oxide liquid (slag) phase. To understand why no halite (MgO) phase has been identified as predicted in **Figure 8b** for the C/A 1.55 slag requires more detailed analysis.

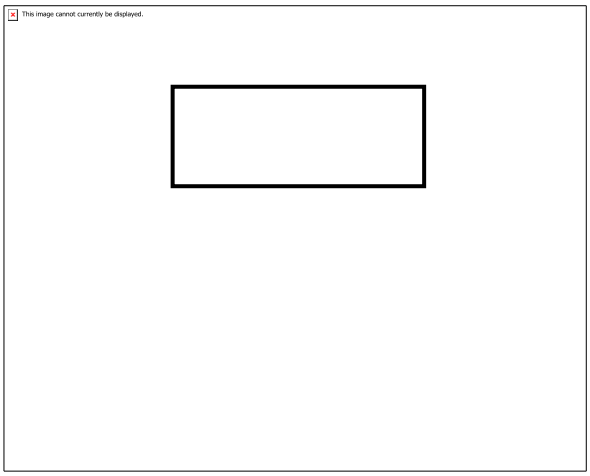

Figure 5a - A cross section micrograph of the spinel-slag C/A 0.98 showing the analyzed areas.

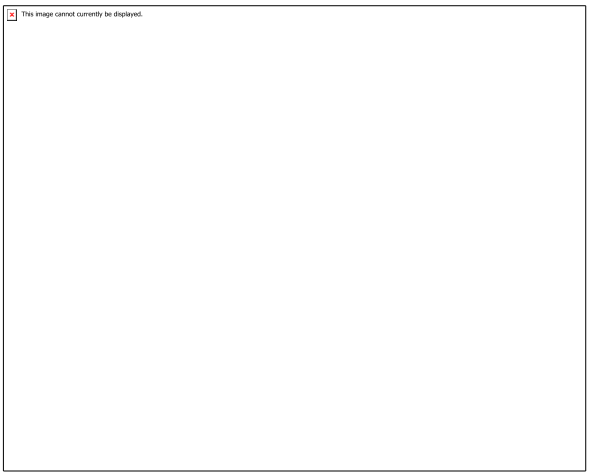

Figure 5b - A micrograph of the spinel-slag C/A 0.98 penetration layer showing the positions of the spot analysis.

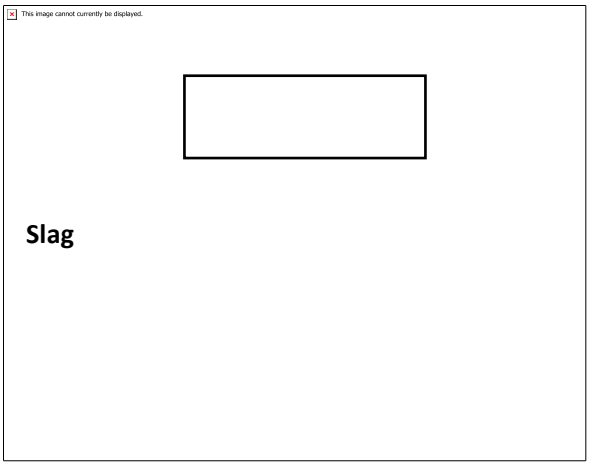

Figure 6a - A cross section micrograph of the spinel-slag C/A 1.25 showing the analyzed areas.

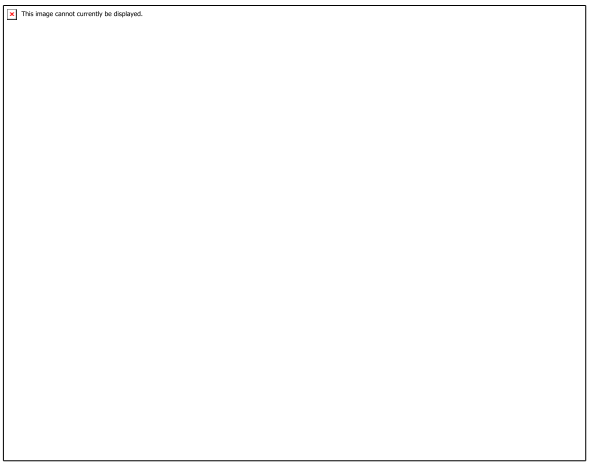

Figure 6b - A micrograph of the spinel-slag C/A 1.25 penetration layer showing the positions of the spot analysis.

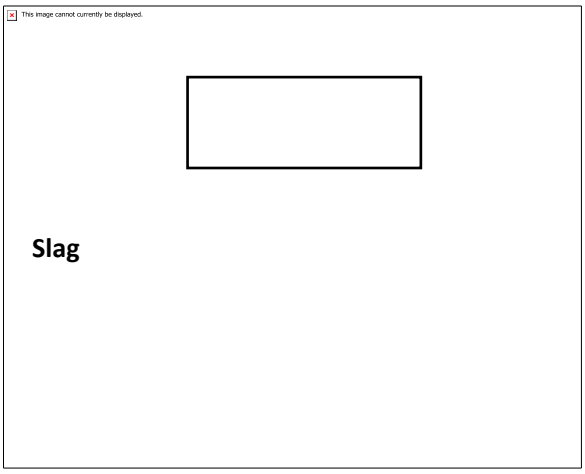

Figure 7a - A cross section micrograph of the spinel-slag C/A 1.55 showing the analyzed areas.

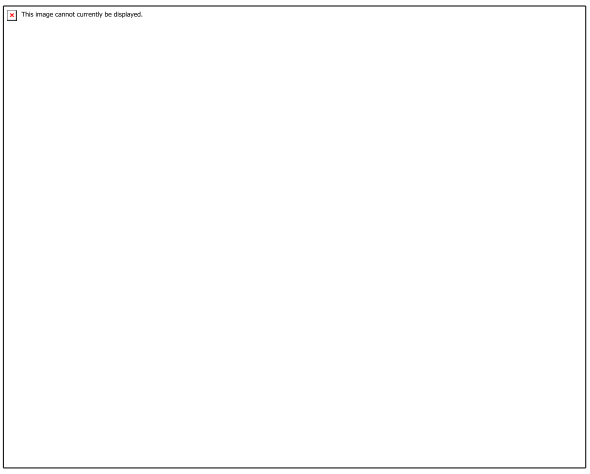

Figure 7b - A micrograph of the spinel-slag C/A=1.55 penetration layer showing the positions of the spot analysis.

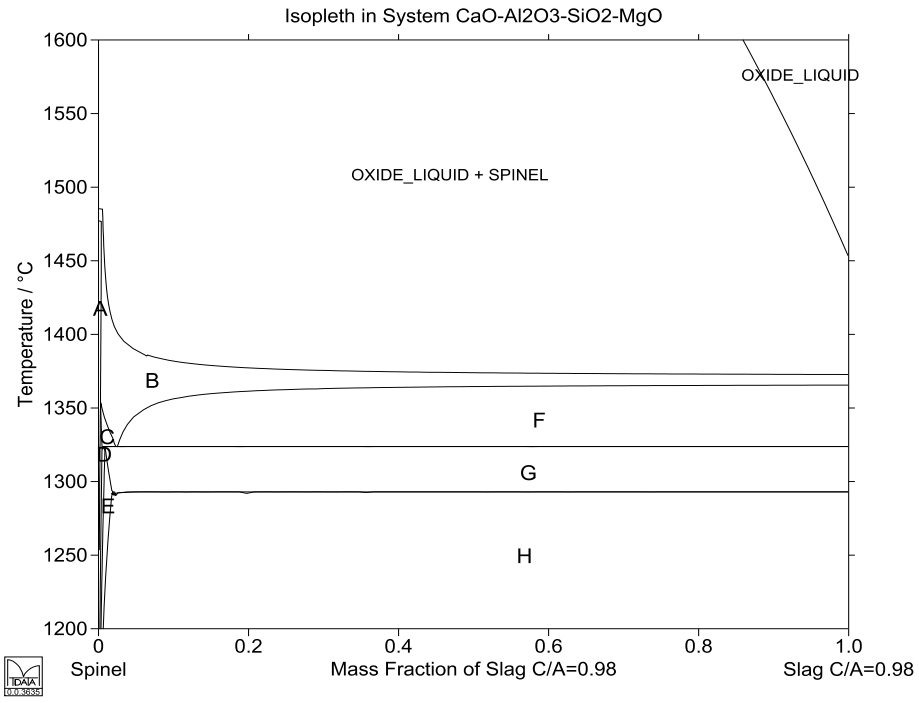

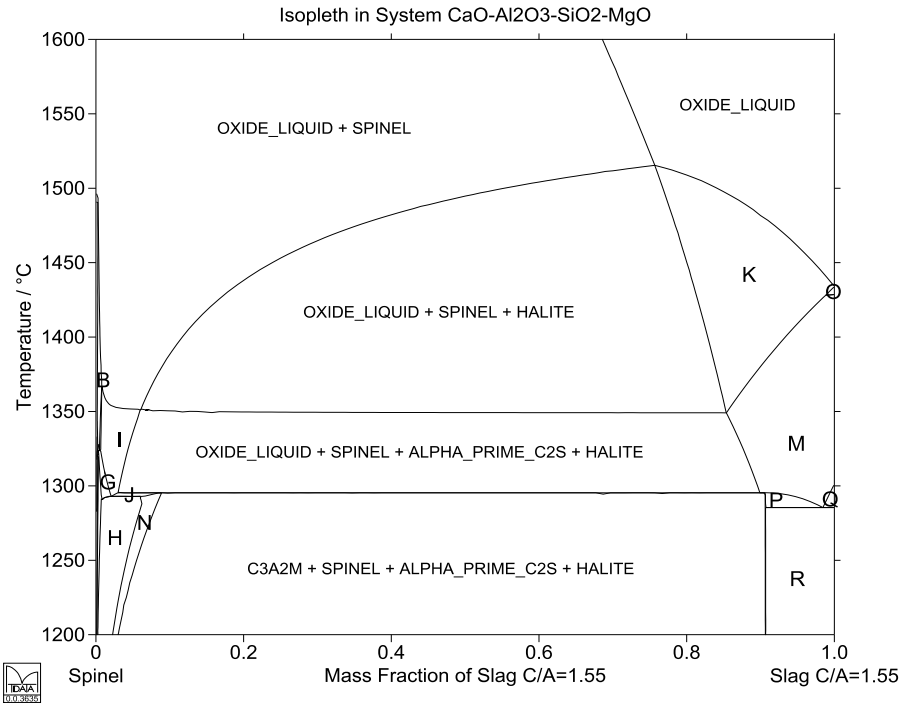

Figure 8: The MTData[19] thermodynamic calculation showing the phase stability in the (a) spinel-slag C/A 0.98 and (b) spinel-slag C/A 1.55 systems. The associated phase fields are shown in table below.

Phase field	Phases present
A	MELILITE + SPINEL
B	OXIDE_LIQUID + MELILITE + SPINEL
C	OXIDE_LIQUID + MELILITE + SPINEL + CA
D	MELILITE + SPINEL + CA + ALPHA_PRIME_C2S
E	SPINEL + CA + ALPHA_PRIME_C2S
F	OXIDE_LIQUID + MELILITE + SPINEL+ ALPHA_PRIME_C2S
G	OXIDE_LIQUID + SPINEL + CA + ALPHA_PRIME_C2S
H	C3A2M + SPINEL + CA + ALPHA_PRIME_C2S
I	OXIDE_LIQUID + SPINEL + ALPHA_PRIME_C2S
J	C3A2M + OXIDE_LIQUID + SPINEL + ALPHA_PRIME_C2S
K	OXIDE_LIQUID + HALITE
L	OXIDE_LIQUID + ALPHA_PRIME_C2S
M	OXIDE_LIQUID + ALPHA_PRIME_C2S + HALITE
N	C3A2M + SPINEL + ALPHA_PRIME_C2S
O	OXIDE_LIQUID + ALPHA_C2S + HALITE

P	C3A2M + OXIDE_LIQUID + ALPHA_PRIME_C2S + HALITE
Q	OXIDE_LIQUID + C3A + ALPHA_PRIME_C2S + HALITE
R	C3A2M + C3A + ALPHA_PRIME_C2S + HALITE

A more detailed thermodynamic analysis of the phases formed at 1500 ^{o}C for the C/A 1.55 is given in **Figure 9**. From **Figure 9** it can be seen that, for mass ratios of $MgAl_2O_4$ to slag up to ~0.76, the amount of spinel is linearly decreasing and inversely proportional to the liquid oxide phase. After this point it is primarily liquid oxide that is stable. The amount of halite (MgO) phase predicted to form, shown in **Figure 9**, reached a maximum of ~ 0.6% by mass and was only stable over a very limited spinel slag mixture range. Given this small value and the limitations of EDS analysis it is not surprising that the MgO phase was not found in the penetration layer of the C/A 1.55 slag.

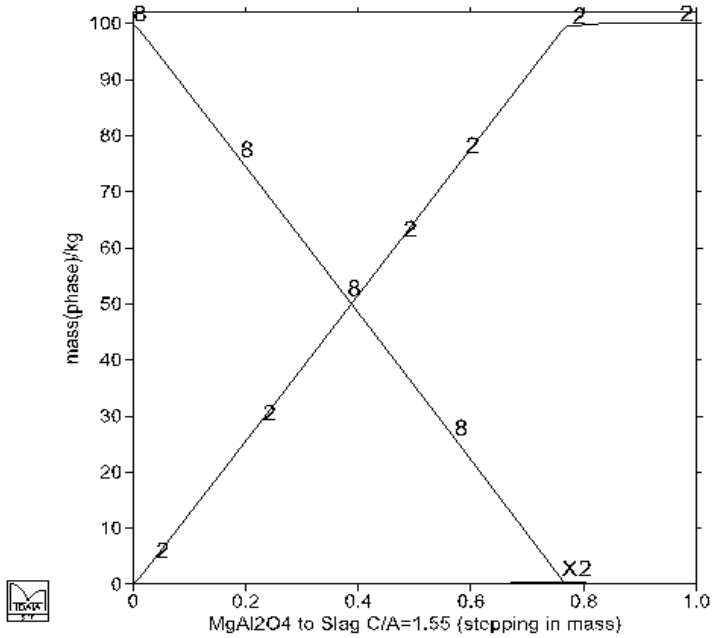

Figure 9: MTData[19] thermodynamic calculations showing the mass of phases present at different $MgAl_2O_4$ to slag C/A 1.55 mass ratios at 1500 ˚C, where 2 = oxide liquid, 8 = spinel and X2 = halite.

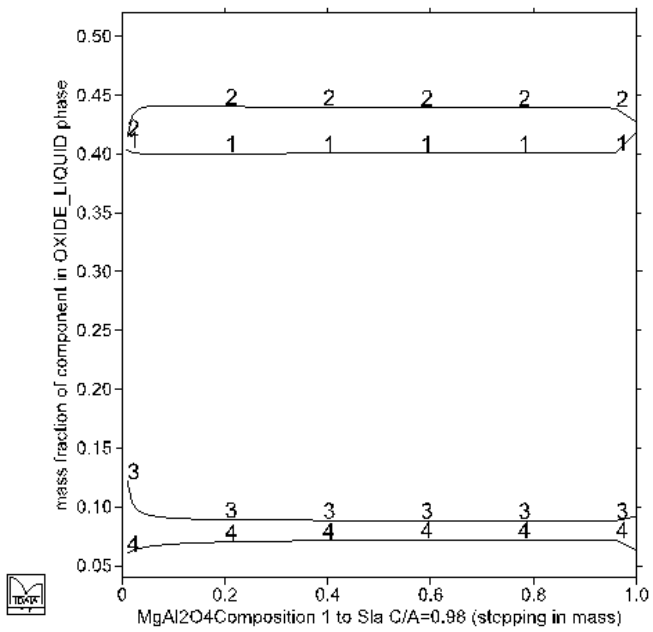

Figure 10: MTData[19] thermodynamic calculations showing the mass fraction of components in the liquid oxide phase at different $MgAl_2O_4$ to slag C/A 0.98 mass ratios at 1500 ˚C where 1=CaO, 2=Al_2O_3, 3=SiO_2, 4=MgO.

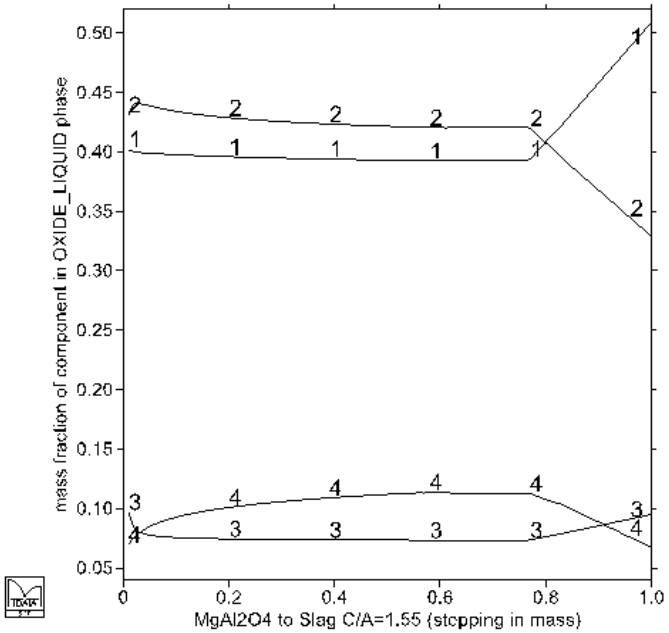

Figure 11: MTData[19] thermodynamic calculations showing the mass fraction of components in the liquid oxide phase at different $MgAl_2O_4$ to slag C/A 1.55 mass ratios at 1500 ˚C where 1=CaO, 2=Al_2O_3, 3=SiO_2, 4=MgO.

The change in mass fraction of the slag components (change in slag composition) of all the stable phases at 1500 ˚C for three slag-spinel substrate systems was also evaluated

using MTData[19]. There was little change predicted in the composition of the spinel and halite phases, as such they are not reproduced here. The slag phase however, and in particular the slag phase in the C/A 1.55 slag-spinel system, was predicted to change (see **Figures 10** to **11**). From the thermodynamic analysis it was expected that there would be an increase in the Al_2O_3 of the slags and a decrease in the CaO of the slag. These changes being modest in C/A 0.98 slag (**Figure 10**) but increasing with C/A ratio of the slag (**Figure 11**). This is broadly consistent with the slag analysis given in **Tables 1** and **2**. Though the C/A 0.98 slag showed little change in the slag composition (**Tables 1** and **2**) before and after the experiment, this is likely due to uncertainties in the EDS analysis, a lower driving force for reaction as the Al_2O_3 and CaO contents of the slag are close to the equilibrium values or some combination of both.

IV. Effect of Cooling Time on the Penetration Layer

Comparison of the of slag-substrate interface at the end of the experiment under the two different cooling regimes (slow cooled in the furnace vs. rapid cooled on the bench top) is given in **Figure 12** for the C/A/ 0.98 slag. From **Figure 12a** and **12b** it can be seen that there is a decrease in the depth of slag penetration from ~190 µm to ~50µm for the slow and rapid cooled samples respectively. A higher magnification image of the area marked with a dashed box in **Figure 12b**, showing the slag penetration is given in in **Figure 12c**. Also shown in **Figure 12c** are the positions of the EDS spot analyses for the spinel (grey phase) and slag (white phase)**.** The respective EDS compositions are given in **Table 4**. The composition of the dark phase represents something close to the original spinel and the white phase is similar to that of the starting slag but is enriched of alumina and depleted of magnesia.

From these data it can be seen that the slag is penetrating/reacting with the spinel substrates even at the short timescales. This is likely to be significant for inclusion removal, where an inclusion has to bond/react with the slag prior to its dissolution in the slag. It is likely this penetration would lead to a stronger bond with the slag and therefore more efficient removal from the liquid steel.

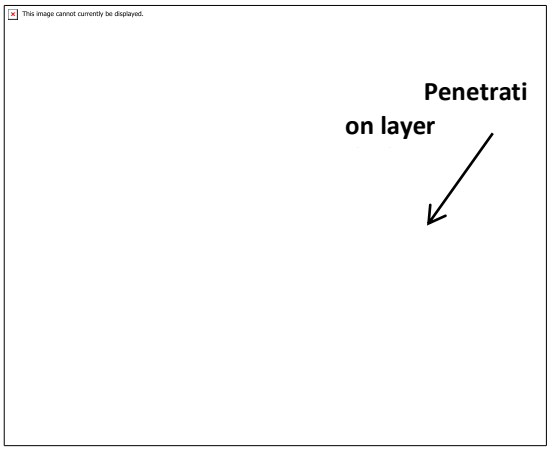

Figure 12a: The thickness of the penetration layer for C/A 0.98 slag under standard measurement conditions and (slow) cooled in the furnace.

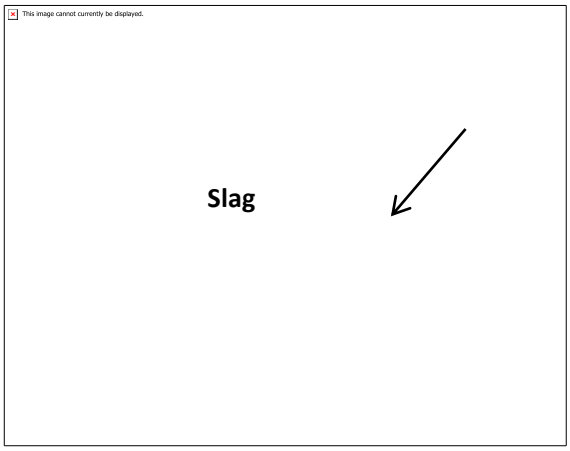

Figure 12b: The thickness of the penetration layer for C/A 0.98 slag where the sample was removed from the furnace in ~60 seconds after time zero and (rapid) cooled on laboratory bench.

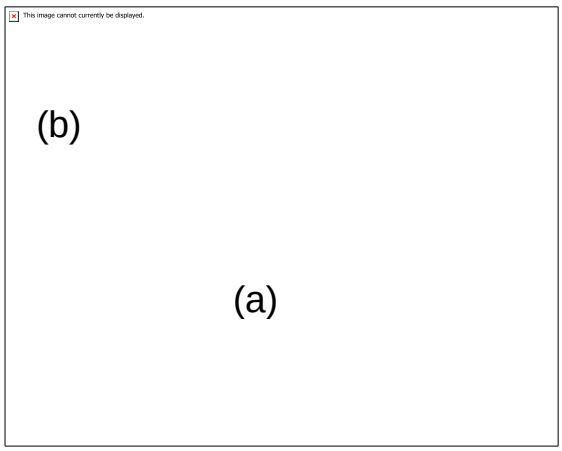

Figure 12c - A higher magnification image of the dashed area marked in Fig 12b, showing the slag penetration and the positions of spot analysis for the spinel-slag C/A 0.98.

Table 4: EDS spot analysis of phases in Figures 12c. Values are in mass%

Location/Phases	CaO	Al_2O_3	SiO_2	MgO
Spinel (grey phases)	0.1	69.7	2.6	27.6
Slag penetration (White phase)	42.6	47.0	7.6	2.8

V. Conclusions

In a study to investigate slag reactivity with inclusions, a series of dynamic wetting measurements and thermodynamic analysis of slags in the CaO-Al_2O_3-SiO_2-MgO system on a $MgAl_2O_4$ spinel substrate was carried out. The key findings were

- The contact angle (θ) of the slag on the substrate decreases rapidly in the first 10s to a plateau value at extended times. The contact angle (θ) decreased from 37.7°, 28.7° and 27° at time zero for the C/A 0.98, C/A 1.25 and C/A 1.55 slags respectively to a slag concentration independent value. After 30s, at the end of the experiment, this value was ~18.1°. This value represents an average of all data reported.
- There was evidence of the slag penetrating the substrate via pores and along grain boundaries, forming a reaction/penetration layer on the substrate. From SEM and EDS analysis this penetrated layer appeared two phase and consisted of something close to the original spinel and a modified slag phase. This was very similar to previous work by the authors on a higher porosity spinel. It would appear at the porosity levels studied 6.7 in the previous work and 1.9% in this work the penetration effects are not a strong function of porosity.
- Thermodynamic modelling of the slag-spinel substrate system was broadly consistent with the EDS analysis of the penetrated layer and post reacted slag.
- The thickness of penetration layer decreased from approximately 190μm to 50μm when the cooling time reduced from 15 min to ~1 min but there is still a reactivity/penetration layer for short contact period in the low porosity (1.9%) spinel.

V. Acknowledgment

The support of BlueScope Steel and the use of the Australian Research Council funded JEOL–JSM6490 LV SEM at the UOW Electron Microscopy Centre is acknowledged.

References

1. J.H. Lowe and A. Mitchell: Clean Steel, Institute of Materials, London, (1995), 223.
2. B. Deo and R. Boom: Fundamentals of Steelmaking Metallurgy, Prentice Hall International, New York, (1993), 254.
3. H. Abdeyazdan, B.J. Monaghan, N. Dogan and M.A. Rhamdhani: High Temperature Processing Symposium, (2013), 44.
4. L. Jonsson and P. Jönsson: ISIJ International, **36**(1996), 1127.
5. L. Zhang, S. Taniguchi and K. Matsumoto: Ironmaking & Steelmaking, **29**(2002), 326.
6. Y. Miki, H. Kitaoka, T. Sakuraya and T. Fujii: ISIJ International, **32**(1992), 142.

7. B.J. Monaghan and L. Chen: Ironmaking and Steelmaking, **33**(2006), 323.
8. B.J. Monaghan, L. Chen and J. Sorbe: Ironmaking & Steelmaking, **32**(2005), 258.
9. K. H. Sandhage & G. J. Yurek: Journal of American Ceramic Society, **74**(1991), 1941.
10. S. Sridhar & A.W. Cramb: Metallurgical and Materials Transactions B, **31**(2000), 406.
11. M. Valdez, K. Prapakorn, A.W. Cramb & S. Seetharaman: Steel Research, **72**(2001), 291.
12. M. Valdez, K. Prapakorn, A.W. Cramb & S. Sridhar: Ironmaking and Steelmaking, **29**(2001), 47.
13. X. Yu, R.J. Pomfret & K.S. Coley: Metallurgical and Materials Transactions B, **28**(1997), 275.
14. K.H. Sandhage & G.J. Yurek: Journal of American Ceramic Society, **71**(1988), 478.
15. K.H. Sandhage & G.J. Yurek: Journal of American Ceramic Society, **73**(1990), 3633.
16. K.H. Sandhage & G.J. Yurek: Journal of American Ceramic Society, **73**(1990), 3643.
17. S. Taira, K. Nakashima & K. Mori: ISIJ International, **33**(1993), 116.
18. K. Ueda: Materials Transactions-JIM, **40**(1999), 989.
19. R.H. Davies, A.T. Dinsdale, J.A. Gisby, J. Robinson & S.M. Martin: Calphad, 26(2002), 229.
20. N. Eustathopoulos, M.G. Nicholas and B. Drevet: Wettability at high temperatures, Elsevier, (1999), 106.
21. A. 1774.5 Method 5: The Determination of Density Porosity and Water Adsorption in Refractories and Refractory Materials, Standards Australia, (2004).
22. J.Y. Choi and H.G. Lee: ISIJ International, **43**(2003), 1348.

Curriculum Vitae

Crystalline slag